Application of zero-valent iron nanoparticles for the removal of aqueous Co2+ ions under various experimental conditions

Article *in* The Chemical Engineering Journal · October 2008

DOI: 10.1016/j.cej.2008.01.024

6 authors, including:

Cagri Üzüm
Surflay Nanotec GmbH
14 PUBLICATIONS **540** CITATIONS
SEE PROFILE

Talal Shahwan
Birzeit University
54 PUBLICATIONS **1,293** CITATIONS
SEE PROFILE

Thomas Bligh Scott
University of Bristol
83 PUBLICATIONS **1,836** CITATIONS
SEE PROFILE

Keith Richard Hallam
University of Bristol
89 PUBLICATIONS **1,604** CITATIONS
SEE PROFILE

ELSEVIER

Chemical Engineering Journal 144 (2008) 213–220

Chemical Engineering Journal

www.elsevier.com/locate/cej

Application of zero-valent iron nanoparticles for the removal of aqueous Co^{2+} ions under various experimental conditions

Ç. Üzüm [a], T. Shahwan [a,*], A.E. Eroğlu [a], I. Lieberwirth [b], T.B. Scott [c], K.R. Hallam [c]

[a] *Department of Chemistry, Izmir Institute of Technology, Urla 35430, Izmir, Turkey*
[b] *Max Planck Institute for Polymer Research, Mainz, Germany*
[c] *Interface Analysis Centre, University of Bristol, 121 St Michael's Hill, Bristol BS2 8BS, United Kingdom*

Received 2 July 2007; received in revised form 4 November 2007; accepted 15 January 2008

Abstract

Nanosized zero-valent iron (nZVI) is increasingly gaining interest as an efficient sorbent for various types of aqueous pollutants. In this study, nZVI was synthesised by the borohydride reduction method, characterised and then examined for the removal of aqueous Co^{2+} ions over a wide range of concentrations, from 1 to 1000 mg/L. The size of nZVI particles was predominantly within the range of 20–80 nm, and only limited oxidation was observed in samples aged for a period of 2 months. The experiments investigated the effects of *V/m* ratio, concentration, contact time, repetitive loading, pH and aging on the extent of retardation of Co^{2+} ions. Iron nanoparticles demonstrated very rapid uptake and large capacity for the removal of Co^{2+} ions. Effective uptake was observed even after a number of repetitive trials. The extent of Co^{2+} uptake increased with the increasing pH. X-ray photoelectron spectroscopy (XPS) indicate that the fixation of Co^{2+} ions takes place through the interaction of these ions with the oxohydroxyl groups on the iron nanoparticle surfaces in addition to spontaneous precipitate formation at high loadings.

Keywords: Nanosized zero-valent iron; Core–shell structure; Co^{2+}

1. Introduction

Iron nanoparticle technology is considered to be among the first generation of nanoscale environmental technologies [1]. Over the past decade, permeable reactive barriers have been developed, as alternatives for the conventional *pump-and-treat* technology, and used to treat groundwater contaminated by different pollutants [2]. In these barriers, zero-valent iron (ZVI) can be used as a reactive material due to its great ability to reduce and stabilise different types of ions. When zero-valent iron is synthesised on the nanoscale, the uptake capacity increased largely due to the increase in surface area and density of reactive sites [3]. An equally important property of nanoscale iron particles is their enormous flexibility for *in situ* applications. Modified iron nanoparticles, such as catalysed and supported nanoparticles, have been synthesised to further enhance the speed and efficiency of remediation [4].

During the last few years, nZVI has been reported to demonstrate effective fixation for various types of metallic ions, including Pb^{2+}, Cr^{6+}, Ni^{2+}, As^{3+}, As^{5+}, Cd^{2+}, Cu^{2+}, Zn^{2+} and Ba^{2+} [5–10]. To our knowledge, the uptake behavior of Co^{2+} on nZVI has not been studied before.

Cobalt is a transition element that is conceived as one of the heavy metals. In addition, cobalt possesses the radioisotope ^{60}Co ($t_{1/2} = 5.3y$) which is extensively used in medicine for cancer treatment as well as for sterilisation purposes. ^{60}Co possesses a relatively long half-life and strong γ radiation ($E_\gamma = 1173.2$, 1332.5 keV). This radioisotope is also important from a radioactive waste point of view, as it is produced by neutron activation of ^{59}Co in nuclear power plants.

In this study, nZVI was synthesised by liquid-phase reduction of $FeCl_2$ and was characterised in terms of its zero-valent content, structure, morphology, zeta potential and surface area. The material was then examined as an adsorbent for aqueous Co^{2+} ions. The uptake capacity of nZVI was investigated over a wide range of initial concentrations of aqueous Co^{2+} solutions, from 1 mg/L up to 1000 mg/L. The uptake experiments included determining the effects of time, *V/m* ratio, repetitive loading,

* Corresponding author. Tel.: +90 232 750 7540; fax: +90 232 750 7509.
E-mail address: talalshahwan@iyte.edu.tr (T. Shahwan).

1385-8947/$ – see front matter © 2008 Elsevier B.V. All rights reserved.
doi:10.1016/j.cej.2008.01.024

pH and aging of the adsorbent on the extent of Co^{2+} retardation. The characterisation techniques included scanning electron microscopy/energy dispersive X-ray (SEM/EDX) analysis, X-ray diffraction (XRD), X-ray photoelectron spectroscopy (XPS), high-resolution transmission electron microscopy (HR-TEM), flame-atomic absorption spectroscopy (FAAS), zeta potential and BET-N_2.

2. Experimental

2.1. Preparation of nZVI

A variety of physical and chemical synthesis techniques are available for nZVI and a summary of these techniques was recently outlined in a review paper on the topic by Li et al. [11]. In this study, nZVI was synthesised using the method of liquid-phase reduction, utilising sodium borohydride as the reducing agent. The procedure followed in this work was primarily based on a previously reported one [12], with some modifications. The experiments were conducted without applying an inert atmosphere or a dispersion agent. In each batch, a sample of $FeCl_2{\cdot}4H_2O$ weighing 17.8 g was dissolved in 50 mL of absolute ethanol and distilled water solution (4:1, v/v). As the reducing agent, 8.47 g $NaBH_4$ was dissolved in 220 mL of distilled water to provide a ~1 M solution. Excess borohydride is typically applied in order to accelerate the reaction and ensure uniform growth of iron particles [4]. The $NaBH_4$ solution was added to the Fe^{2+} solution drop wise (40–50 drops/min) while stirring the reaction mixture well. The resulting reaction occurs as below:

$$Fe^{2+} + 2BH_4{}^- + 6H_2O \rightarrow Fe^0 + 2B(OH)_3 + 7H_2\uparrow$$

Black particles of nZVI appeared immediately after introducing the first drop of $NaBH_4$ solution. Further mixing for 20 min was allowed following the addition of $NaBH_4$ solution. Black iron powder was separated from the solution by vacuum filtration using Whatman (blue band) filter papers. The solid was then washed at least three times with 99% absolute ethanol. This washing step appeared to be critical in stabilising nZVI against immediate oxidation, as samples washed with deionised water showed faster oxidation when exposed to the atmosphere. Finally, the powder was taken into a watch glass and dried in an oven at 75 °C overnight. It must be noted here that during the earlier trials of nZVI synthesis, when the iron powder was dried in an evacuated oven, the sample ignited at once upon exposure to atmospheric oxygen. Therefore, the drying step was always performed in the oven without air evacuation. The obtained powder had a black colour and no significant change in colour was detected for samples stored under normal conditions for a period of 2 months.

In order to identify the iso-electric-point (IEP) of the iron nanoparticles, zeta potential was measured for a series of iron suspensions having adjusted pH values in the range 6.0–12.0. The measurements were conducted at a concentration of 0.1 g/L using a Zeta-Meter 3.0 instrument.

2.2. Uptake experiments

All the Co^{2+} solutions were prepared by dissolving appropriate amounts of $CoCl_2{\cdot}5H_2O$ in ultra-pure water (18 MΩ). In the experiments performed to investigate the effect of *V/m* ratio (volume of solution/mass of sorbent), the applied ratios were 50, 100, 150 and 200 mL/g. This was achieved through adding 0.200, 0.100, 0.067 and 0.050 g doses of nZVI into 10 mL of 1, 5, 50 or 1000 mg/L Co^{2+} solutions and shaking for 24 h.

To elucidate the time required to achieve equilibrium of uptake, solutions of Co^{2+} with concentrations of 10, 100 and 1000 mg/L were shaken for 5 min, 10 min, 20 min, 40 min, 1 h, 2 h, 4 h and 24 h. In each sample, 10 mL of solution was added to 0.20 g of sorbent. The extent of desorption was investigated by exposing the Co-loaded samples of iron nanoparticles to distilled water for different shaking periods. Four mixtures, shaken for 5 min, 30 min, 2 h and 24 h, respectively, were then centrifuged and the liquid phases were transferred into clean falcon tubes for concentration analysis.

The extent of uptake as a function of initial concentration was studied at Co^{2+} concentrations of 1, 5, 10, 50, 100, 250, 500 and 1000 mg/L. In these experiments, 0.050 g samples of nZVI were separately added to 40 mL aliquots to have volume/mass (mL/g) ratios of 800. The mixtures were then shaken for 24 h.

In order to check the effect of repetitive loading on the reactivity of the nZVI, 0.20 g samples of nZVI were repeatedly exposed to 10.0 mL aliquots of fresh Co^{2+} solutions having initial concentrations of 1, 5, 100 or 1000 mg/L. Each of the repetitive experiments was conducted for 45 min of shaking. The mixtures were then centrifuged, the supernatant solutions collected as explained below and fresh Co^{2+} solutions added to the solid. Each solid was exposed to eight repetitive trials of uptake.

A set of experiments was also performed at the initial Co^{2+} concentration of 1000 mg/L in order to check the effect of aging of nZVI on its scavenging ability. In each experiment, 10 mL of Co^{2+} solution were contacted with 0.2 g nZVI for a period of 24 h.

In the pH-uncontrolled experiments performed using nZVI, the pH varied between 6.4 and 8.7 depending on the applied concentration of Co^{2+}; the higher the concentration the lower the pH. The chemical speciation analysis of aqueous cobalt ions under different pH conditions was performed using visual MINTEQ software using input conditions corresponding to various initial concentration, temperature, pH and ionic strength values. The results showed that up to pH values of 8–9, the dominant chemical form of Co in aqueous media is Co^{2+}. Above pH 9, forms like $CoOH^+$ and $Co(OH)_2$(aq) become increasingly effective. Depending on this, it is apparent that, within the experimental conditions of this study, the dominant form of cobalt in aqueous media is Co^{2+}.

In order to reveal the effect of pH, the pH of the mixtures were adjusted to 4.0, 6.0, 8.0 and 10.0 at the start of mixing. In these experiments, 20 mL of 1000 mg/L Co^{2+} solution were mixed with 0.05 g of nZVI in the presence of 0.01 M NaCl applied to stabilise the ionic strength of the medium. The pH was adjusted by adding droplets of 3.0 M or 1.0 M HCl or NaOH solutions. The mixtures were then shaken for 24 h.

In each of the above experiments, the mixtures were contained in 50 mL polypropylene centrifuge tubes. Following shaking, these mixtures were centrifuged; the supernatant solutions were collected and acidified to 1% (v/v) by concentrated nitric acid. The filtrate was then analysed for Co content with flame AAS using a Thermo Elemental SOLAAR M6 Series atomic absorption spectrometer with an air–acetylene flame. The solid samples were characterised using XRD and SEM/EDX prior to and following the uptake process. XRD analysis was performed using a Philips X'pert Pro diffractometer with Cu Kα radiation (λ = 1.54 A). Patterns were recorded from each sample over a 2-theta range of 10–90°. SEM/EDX analysis was done using a Philips XL-30S FEG instrument. The solid samples were first sprinkled onto adhesive carbon tapes supported on metallic disks. Images of the sample surfaces were then recorded at different magnifications. The EDX analysis was performed at randomly selected areas on the solid surfaces to elucidate the atomic distribution on the surface of the adsorbents.

The nZVI samples were also analysed using HR-TEM with a Tecnai F20 instrument located at the Max Planck Institute for Polymer Research. The instrument was operated at 200 kV acceleration voltage. Prior to analysis, nZVI was dispersed in ethanol using an ultrasonic bath and a drop of the dispersion was applied to a holey carbon TEM support grid. Excess solution was blotted off using a filter paper.

For XPS analysis, the samples were mounted in Al holders and analysed under high vacuum (<1×10^{-7} mbar) in a Thermo VG Scientific X-ray photoelectron spectrometer equipped with a dual anode (Al Kα 1486.6 eV and Mg Kα 1253.6 eV). Al Kα radiation was used 400 W (15 kV) for the analyses. High resolution scans were acquired with 30 eV pass energy and 200 ms dwell time while wide scan survey spectra were acquired with 100 eV pass energy and 200 ms dwell time. Data analysis was carried out using Dayta Systems' Pisces software.

3. Results and discussion

The XRD diffractogram of freshly synthesised nZVI is shown in Fig. 1a. The figure indicates that iron is mainly in its Fe^0 state, characterised by the basic reflection appearing at a 2-theta value of 44.9°. Signals of the iron oxides (haematite, Fe_2O_3, or magnetite, Fe_3O_4) were not observed in the XRD patterns of fresh samples. Samples of iron nanoparticles stored for several weeks showed weak oxide signals at 36° 2-theta in their XRD patterns. The pattern of a sample 3 weeks after its preparation is given in Fig. 1b. The features of iron oxide became more distinct in nZVI samples aged for 2 months (Fig. 1c). It must be noted that the extent of oxidation of iron might not be fully elucidated by XRD examination solely because of the limitations in detection level of this technique. This topic was considered further in light of HR-TEM findings as given below.

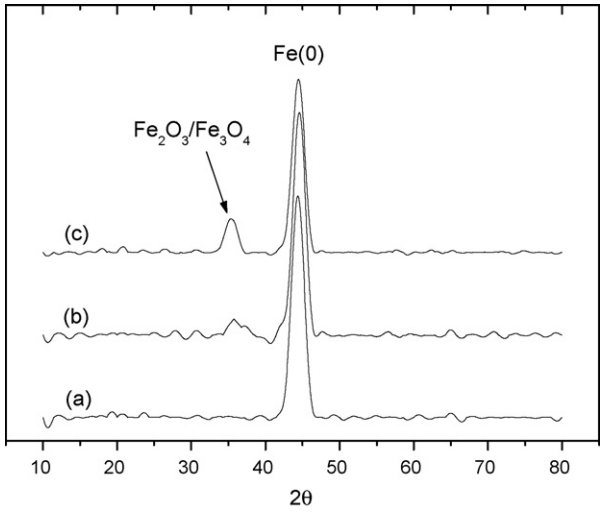

Fig. 1. XRD patterns of nZVI: (a) fresh; (b) after 3 weeks; and (c) 2 months after synthesis.

Typical SEM images of the synthesised iron nanoparticles are shown in Fig. 2. The fresh iron particles appear to have size distribution within 20–80 nm (Fig. 2a), demonstrating the characteristic chain-like morphology. Aggregation of the nanoparticles is reported to be caused by the large surface area and magnetic dipole–dipole interactions of the individual particles [11]. SEM analysis of a 2-month aged sample of nZVI (Fig. 2b) showed that the chain-like structure was still dominant but indicated also the presence of some larger floc aggregates, stemming possibly from the enhancement in oxide formation.

Literature resources indicate that iron nanoparticles possess a core–shell structure, in which the shell represents the oxidised part that surrounds the Fe^0 core and preserves it against fur-

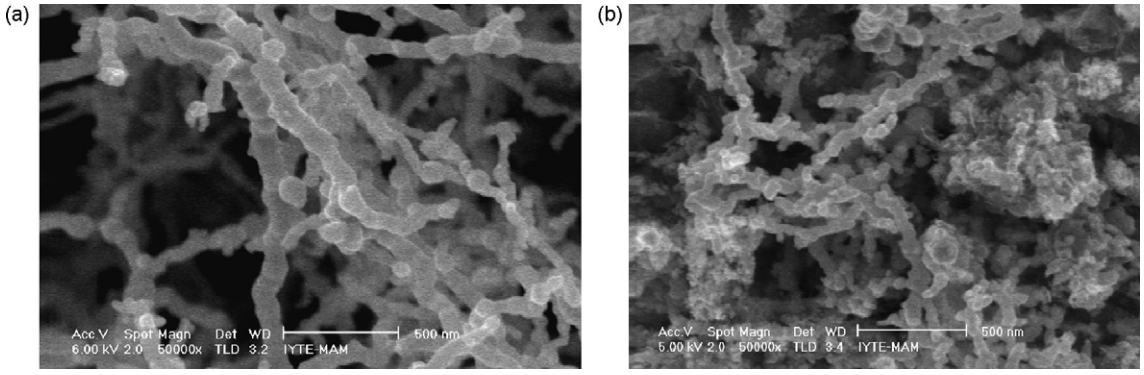

Fig. 2. Typical SEM images of nZVI: (a) a freshly prepared sample and (b) a sample aged for 2 months.

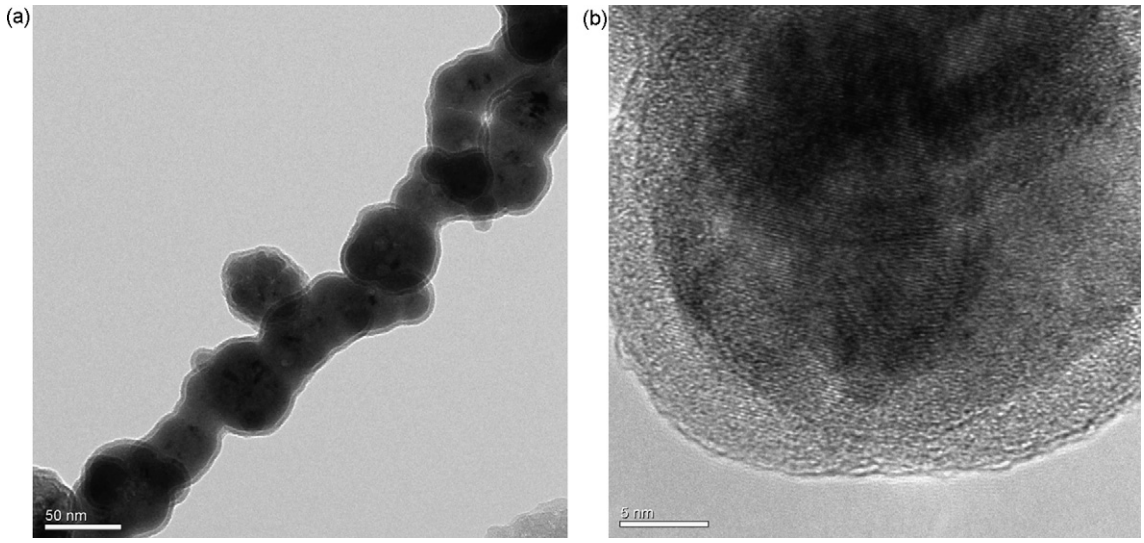

Fig. 3. HR-TEM images of nZVI fresh at different magnifications.

ther oxidation [e.g. 1,3,6,7,9]. As shown in Fig. 3, the HR-TEM analysis performed in this study supports this view with the shell being about 3–5 nm thick, in line with previously reported values. The absence of high-resolution fringes in the shell image indicates that the shell is amorphous.

The measurements of zeta potential at different pH values showed that the iso-electric-point of iron nanoparticles occurred around 8.1–8.2. This is in line with the value reported earlier by other authors [1]. According to surface area analysis, the BET surface area of iron nanoparticles is 14.2 m^2/g, and the Langmuir surface area is 51.4 m^2/g. The same analysis indicated also that the adsorption average pore width (4*V*/*A* by BET) is 38.8 Å, and that the *t*-plot micropore volume is 0.01138 cm^3/g. It is reported that a surface area measured on a dry basis is unlikely to reflect the actual available area in solution because of the tendency of nZVI particles to aggregate inside solution [3].

Kinetic experiments were carried out to determine the time required to reach equilibrium. The results showed that equilibrium was achieved within 10 min of contact at the initial concentration of 10 and 100 mg/L. When the initial concentration was raised to 1000 mg/L, about half an hour was required to achieve equilibrium. Such a rapid uptake is indicative that the sites on nZVI are readily accessible for Co^{2+} ions. The desorption behavior of initially fixed Co^{2+} ions was studied at different periods extending from 5 min up to 24 h. In general, an increase in the released amounts of Co^{2+} ions occurred as the shaking time increased. At the end of 24 h, the values of % desorption of initially fixed Co^{2+} ions were 3.6, 5.6 and 17.0 for samples prepared at the initial concentrations of 10, 100 and 1000 mg/L. The values of % desorption were calculated using the concentrations of Co^{2+} released from iron nanoparticles into solution, relative to the amount of the ion originally fixed at the stage of uptake.

The next experiments were conducted to reveal the effect of the *V*/*m* ratio and the results are presented in Table 1. According to these, at initial concentrations of 1, 5 and 50 mg/L, almost complete removal of Co^{2+} ions was achieved regardless of the applied *V*/*m* condition. When the initial concentration was raised to a value as high as 1000 mg/L, however, a gradual decrease in % uptake was observed to accompany the increase in *V*/*m* ratio. The results provided in Table 1 indicate that, at high concentration, the larger quantity of adsorbent leads to higher removal and also that nZVI is so efficient that raising the *V*/*m* ratio fourfold (or decreasing the amount of nZVI by a factor of 4) leads to a decrease of only about 20% in the percentage removal by nZVI.

In order to study the variation of the uptake capacity of nZVI with initial concentration, a separate set of experiments was performed in which the *V*/*m* ratio was raised to a value as high as 800 mL/g. The variation of equilibrium concentration in solu-

Table 1
Values of % uptake of Co^{2+} on nZVI obtained for different initial concentrations and different *V*/*m* ratios

Initial concentration (mg/L)	Volume (mL)	nZVI (g)	*V*/*m* (mL/g)	% Uptake
	10	0.20	50	>99
	10	0.10	100	>99
1	10	0.67	150	98
	10	0.05	200	>99
	40	0.05	800	99
	10	0.20	50	>99
	10	0.10	100	>99
5	10	0.67	150	98
	10	0.05	200	97
	40	0.05	800	98
	10	0.20	50	>99
	10	0.10	100	>99
50	10	0.67	150	98
	10	0.05	200	99
	40	0.05	800	96
	10	0.20	50	95
	10	0.10	100	85
1000	10	0.67	150	73
	10	0.05	200	74
	40	0.05	800	22

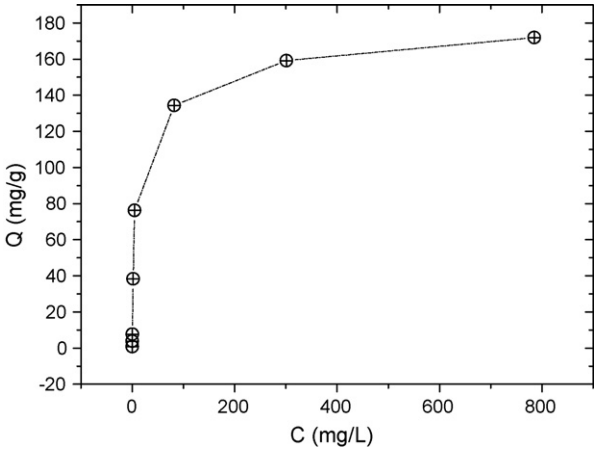

Fig. 4. The uptake isotherm of Co^{2+} on nZVI at a *V*/*m* ratio of 800 mL/g.

tion, *C* (mg/L), with that on the solid *Q* (mg/g), is shown by the isotherm presented in Fig. 4. Up to 100 mg/L initial concentration, nZVI seems to be very effective in Co^{2+} fixation. Beyond the initial Co^{2+} concentration of 250 mg/L, a saturation stage is approached. At the highest studied initial concentration, the amount of Co^{2+} on iron nanoparticles was 172.0 mg/g. This value seems to be larger than the uptake capacity values reported earlier for various sorbents, as shown in Table 2. It should be stressed, however, that the values given in the table originate from different studies in which the experimental conditions might not match those applied in the current study and, as such, that the comparison made here aims at showing the high uptake potential of iron nanoparticles rather than establishing a quantitative scale of efficacy among different sorbents.

In order to test the effect of aging on the reactivity of nZVI, experiments were performed using freshly produced nZVI in addition to samples aged for the periods of 4, 15, 25 and 40 days. The results indicated that iron nanoparticles have largely

Table 2
A comparison of Co^{2+} uptake capacities by different sorbent materials

Sorbent	Uptake capacity (mg/g)	Reference
nZVI	172.0	This study
Activated carbon	13.88	[13]
Vermiculite	49.49	[14]
IRN77 resin	86.17	[15]
Bentonite	125.9	[16]
Anaerobic granular sludge	18.76	[17]
Hydroxyapatite	20.19	[18]
TVEX–PHOR resin	8.7	[19]

Table 3
Values of the equilibrium concentrations and % uptake of Co^{2+} ions on nZVI samples kept for different aging times before being applied as adsorbents

Sample aging	*C* (mg/L)	*Q* (mg/g)	% Uptake
Fresh	20.0	49.0	97
4 days	63.2	46.8	94
15 days	88.4	45.6	91
25 days	43.6	47.8	96
40 days	113	44.4	89

In each trial, 10 mL of 1000 mg/L Co^{2+} solution were contacted with 0.2 g nZVI for a period of 24 h.

retained their reactivity towards Co^{2+} ions even 40 days after preparation. The results expressed in terms of % uptake are provided in Table 3. According to these findings, the percentage removal of Co^{2+} ions varies within less than 10% among the aged nZVI, and even for nZVI samples that were aged for 40 days the uptake is as high as 89%. The extent of loss of reactivity with aging is closely related to the uptake mechanism, which is discussed below, and further work on nZVI samples aged for longer periods is required for a detailed assessment of the topic.

The high uptake capacity demonstrated by nZVI motivated testing of the effect of repetitive loading on the reactivity of

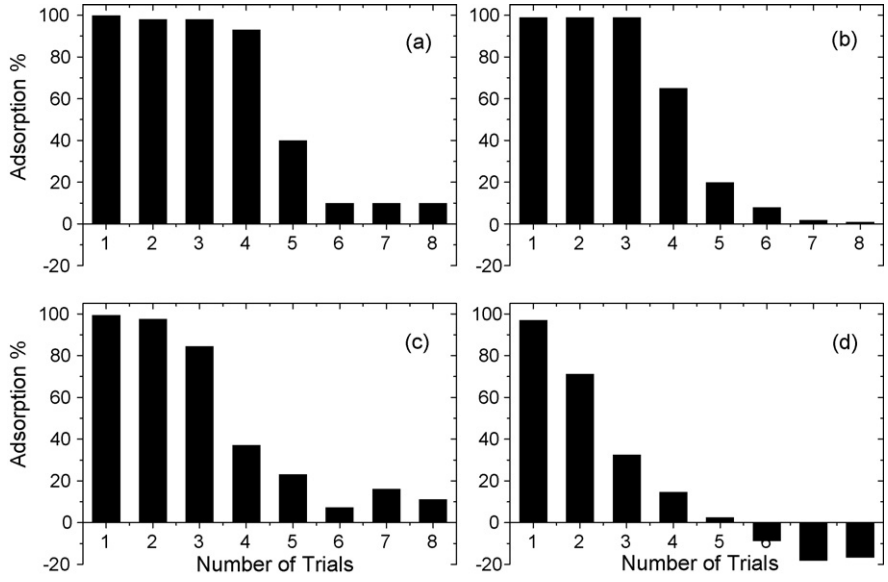

Fig. 5. Variation of the % uptake with the number of applications of the same nZVI samples at the initial Co^{2+} concentrations of: (a) 1 mg/L; (b) 5 mg/L; (c) 100 mg/L; and (d) 1000 mg/L.

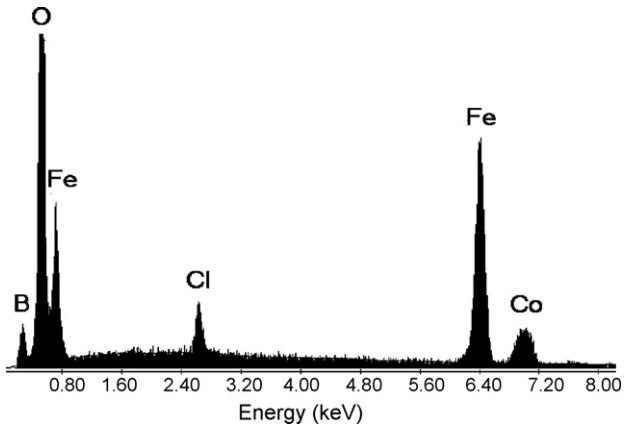

Fig. 6. A typical EDX spectrum of nZVI after the uptake of Co^{2+} ions at the initial concentration of 1000 mg/L. The Co peak might contain contribution from Fe Kβ.

this adsorbent. The results are demonstrated in Fig. 5 at initial Co^{2+} concentrations of 1, 5, 100 and 1000 mg/L. The figure shows the change in % uptake with the number of applications of the same sample of nZVI. The decrease in the uptake capacity of the repeatedly applied iron nanoparticles is concentration-dependent. The decrease is most drastic for the highest initial concentration, as expected. The negative values of the % uptake after the fifth trial in Fig. 5d possibly stem from partial desorption of previously fixed Co^{2+} ions.

Energy dispersive X-ray (EDX) analysis was used to evaluate the elemental content of nZVI following the uptake of Co^{2+} ions. A typical EDX spectrum recorded for Co^{2+}-loaded iron nanoparticles, exposed to an initial concentration of 1000 mg/L at *V*/*m* ratio of 50, is shown in Fig. 6. Due to the detection limit of EDX, elemental evaluation at lower Co^{2+} initial concentrations was not possible. For this sample, 95% uptake was achieved (see Table 1), which corresponds to a Co^{2+} concentration of 47.5 mg/g of nZVI. EDX spectra were collected from randomly selected points on the surface and indicated the presence of Cl (originating from $FeCl_2$) and B (caused by $NaBH_4$) in addition to O, Fe and Co in the structure. According to EDX quantification, the atomic percentage of Co on the iron surface was within the range 4.5–5.9 and the average atomic ratio of Co/Fe was 0.16. It must be noted that there is a possibility for the overlap of EDX lines of Co Kα with Fe Kβ due to their close energies, therefore the given values must be carefully viewed.

In a pioneering study that surveyed the XPS spectra for a variety of metal ions upon sequestration by nZVI, Li and Zhang reported that nZVI has the ability to remove metal ions from aqueous solution by multiple mechanisms thought to be in direct dependence on the core–shell structure of the nanoparticles [9]. These mechanisms are reported by the same authors to include electrostatic adsorption, complex formation, reduction and precipitation, the contribution of each of which is dependent on the standard electrode potential of the metal ion and the operating experimental conditions, in particular pH of the medium [9]. Taking into consideration that the standard reduction potential of Co^{2+} (= −0.28 V, 298 K) is somewhat larger than that of Fe^{2+} (= −0.44 V, 298 K), the removal of aqueous Co^{2+} might be expected to take place to a certain extent through a redox reaction in which insoluble Co^0 is produced. In earlier investigations, the oxidation–reduction mechanism of uptake was reported to be effective for a number of ions that are higher in the electrochemical series than Fe^{2+}, such as Pb^{2+} and Cr^{6+} [5], Ni^{2+} [6], As^{3+} and As^{5+} [7,8] and Cu^{2+}, Ni^{2+} and Ag^{+} [9]. However, our XPS analysis did not confirm that sorbed cobalt was present in its zero-valent form. According to this analysis, the recorded Co $2p_{3/2}$ peaks were located at 781.2 ± 0.1 eV and were asymmetric to the high binding energy side. This value occurs in between the values reported earlier to correspond to Co^{2+} in CoO (780.0 ± 0.2 eV for the $2p_{3/2}$ line) [20,21], and to Co^{2+} in $Co(OH)_2$ (782.0 ± 0.1 eV for the $2p_{3/2}$ line) [22]. Both lines are readily discerned from that corresponding to metallic cobalt, Co^0 (778.0 ± 0.2 eV for the Co$2p_{3/2}$ line) [20,23]. Based on this, it could be suggested that Co^{2+} ions did not undergo reduction upon their fixation by iron nanoparticles but were fixed by the hydroxyl groups at the surface of the shell of iron nanoparticles or simply precipitated on that surface in the form of $Co(OH)_2$. As reported earlier [9], iron nanoparticles in contact with aqueous solution develop FeOOH groups as a result of surface hydroxylation and subsequent dehydration of the exposed shell. The development of such groups is evident in the XPS spectrum provided in Fig. 7 for a sample of iron nanoparticles at the end of uptake. The recorded Fe 2p photoelectron profile was very similar to that attributed to Fe in ferrioxyhydroxide (FeOOH) with the Fe $2p_{3/2}$ line centred at 711.7 ± 0.1 eV binding energy [23].

As given earlier in this text, the iso-electric-point of iron nanoparticles occurred at a pH of 8.1–8.2. Thus, when the pH of the medium is higher than the IEP, the surface will be negatively charged and consequently attract the positively charged Co^{2+} ions. The pH variation with time at different initial concentrations is shown in Fig. 8. According to the obtained values, up to the initial Co^{2+} concentration of 100 mg/L the pH values appear to be higher than the IEP throughout the mixing time. Within this concentration range, significant contribution of electrostatic attractions and surface complex formations between

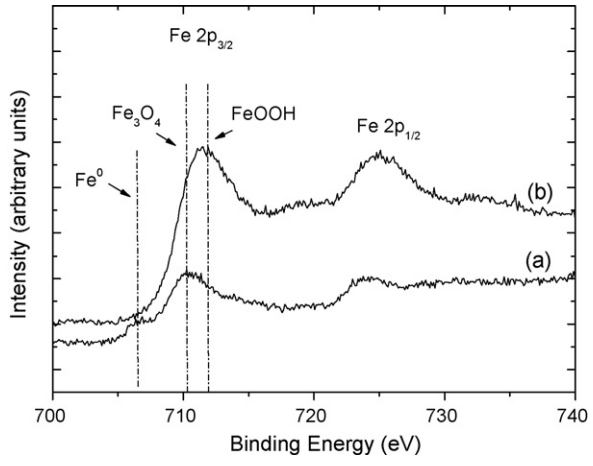

Fig. 7. XPS spectra showing Fe peaks for: (a) an iron standard; and (b) a sample of iron nanoparticles at the end of mixing with Co^{2+} aqueous solution.

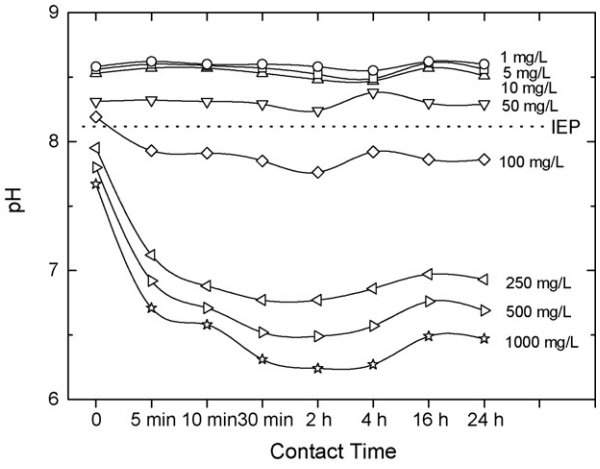

Fig. 8. pH variation with time at different initial Co^{2+} concentrations.

Co^{2+} ions and surface groups on the iron nanoparticles seems to be plausible. In the case of higher initial Co^{2+} concentrations, the pH is seen to drop below the IEP throughout the course of mixing. As long as the over-saturation conditions are met, the contribution of spontaneous precipitation of $Co(OH)_2$ might be more pronounced in comparison to sorption processes.

In order to assess further the importance of pH on the extent of Co^{2+} retention by nZVI, separate sets of experiments were carried out in which the initial pH values were adjusted in the range 4.0–10.0 and the initial concentration of Co^{2+} ions was kept at the highest studied value, i.e. 1000 mg/L. One set of experiments was performed with Co^{2+} solutions prepared in distilled water while in the other 0.01 M NaCl was applied as a background electrolyte. The results are given in Table 4. While a small increase in the % uptake of Co^{2+} ions took place when the pH was raised from 4.0 to 6.0, a great increase in the extent of uptake occurred when the pH was increased from 6.0 through 8.0 up to 10.0, where almost complete removal was achieved. This drastic change is pointing to the role of protonation/deprotonation of the hydroxyl species on the surface of iron nanoparticles, in addition to precipitation of cobalt hydroxide in the fixation of Co^{2+} ions.

Table 4
Initial and final pH values and the corresponding % uptake of Co^{2+} ions on nZVI samples

	Initial pH	Final pH	% Uptake
(i)	4.0	6.2	15.1
	6.0	6.4	17.3
	8.0	6.9	87.8
	10.0	9.2	99.0
(ii)	4.0	4.7	14.3
	6.0	4.9	25.1
	8.0	7.0	96.7
	10.0	9.2	>99.9

In each trial, 20 mL of 1000 mg/L Co^{2+} solution were contacted with 0.05 g nZVI for a period of 24 h:(i) the experiments performed in distilled water; and (ii) the experiments performed using 0.01 M NaCI as background electrolyte.

4. Conclusions

Nanoparticles of zero-valent iron synthesised in an ethanol–water medium showed a significant stability against atmospheric conditions. In line with previous reports about the topic, the particles possessed a core–shell structure, with diameter that is predominantly in the range of 20–80 nm, and appeared to form chain-like aggregates. Under various sets of experimental conditions, nZVI demonstrated high retention capacity and very rapid uptake kinetics in the removal of aqueous Co^{2+} ions. Aging of nZVI up to 2 months caused small changes in the reactivity of the material, which also demonstrated effective retardation of Co^{2+} ions even after a number of repetitive trials. Increasing the pH lead to an increase in the amount of fixed Co^{2+} ions. The mechanism of uptake seems to be related to the speciation of surface oxohydroxyl groups on the nZVI surface and no evidence of a redox mechanism was detected.

Acknowledgements

This work was sponsored by the 2006 IYTE 13 fund provided by Izmir Institute of Technology. The authors would like to thank the research specialist Sinan Yılmaz, for help with the AAS measurements, and the Center of Material Research at Izmir Institute of Technology (İYTE-MAM), for assistance in the SEM and XRD measurements.

References

[1] Y. Sun, X. Li, X.J. Cao, W. Zhang, H.P. Wang, Characterization of zero-valent iron nanoparticles, Adv. Colloid Interface Sci. 120 (2006) 47–56.
[2] D.W. Blowes, C.J. Ptacek, S.G. Benner, W.T. McRae Che, T.A. Bennett, R.W. Puls, Treatment of inorganic contaminants using permeable reactive barriers, J. Contam. Hydrol. 45 (2000) 123–137.
[3] J.T. Nurmi, P.G. Tratnyek, V. Sarathy, D.R. Bear, J.E. Amonette, K. Peacher, C. Wang, J.C. Linehan, D.W. Matson, R.L. Penn, M.D. Driessen, Characterization and properties of metallic iron nanoparticles: spectroscopy, electrochemistry, and kinetics, Environ. Sci. Technol. 39 (2005) 1221–1230.
[4] W.-X. Zhang, Nanoscale iron particles for environmental remediation: an overview, J. Nanopart. Res. 5 (2003) 323–332.
[5] S.M. Ponder, J.G. Darab, T.E. Mallouk, Remediation of Cr(VI) and Pb(II) aqueous solutions using nanoscale zero-valent iron, Environ. Sci. Technol. 34 (2000) 2564–2569.
[6] X.Q. Li, W.-X. Zhang, Iron nanoparticles: the core–shell structure and unique properties for Ni(II) sequestration, Langmuir 22 (2006) 4638–4642.
[7] S.R. Kanel, B. Manning, L. Charlet, H. Choi, Removal of arsenic(III) from groundwater by nanoscale zero-valent iron, Environ. Sci. Technol. 39 (2005) 1291–1298.
[8] S.R. Kanel, J.M. Greneche, H. Choi, Arsenic(V) removal from groundwater using nano scale zero-valent iron as a colloidal reactive barrier material, Environ. Sci. Technol. 40 (2006) 2045–2050.
[9] X.-Q. Li, W.-X. Zhang, Sequestration of metal cations with zerovalent iron nanoparticles—a study with high resolution X-ray photoelectron spectroscopy (HR-XPS), J. Phys. Chem. C 111 (2007) 6939–6946.
[10] O. Çelebi, Ç. Üzüm, T. Shahwan, H.N. Erten, A radiotracer study of the adsorption behavior of aqueous Ba^{2+} ions on nanoparticles of zero-valent iron, J. Hazard. Mater. 148 (2007) 761–767.
[11] L. Li, M. Fan, R.C. Brown, J.V. Leeuwen, J. Wang, W. Wang, Y. Song, P. Zhang, Synthesis, properties, and environmental applications of nanoscale iron-based materials: a review, Crit. Rev. Environ. Sci. Technol. 36 (2006) 405–431.

[12] W. Wang, Z.-H. Jin, T.-L. Li, H. Zhang, S. Gao, Preparation of spherical iron nanoclusters in ethanol–water solution for nitrate removal, Chemosphere 65 (2006) 1396–1404.
[13] E. Demirba, Adsorption of cobalt(II) ions from aqueous solution onto activated carbon prepared from hazelnut shells, Adsorpt. Sci. Technol. 21 (2003) 951–963.
[14] M.G. da Fonseca, M.M. de Oliveira, L.N.H. Arakaki, J.G.P. Espinola, C. Airoldi, Natural vermiculite as an exchanger support for heavy cations in aqueous solutions, J. Colloid Interface Sci. 285 (2005) 50–55.
[15] S. Rengaraj, S.H. Moon, Kinetics of adsorption of Co(II) removal from water and wastewater by ion exchange resins, Water Res. 36 (2002) 1783–1793.
[16] T. Shahwan, H.N. Erten, S. Unugur, A characterization study of some aspects of the adsorption of aqueous Co^{2+} ions on a natural bentonite clay, J. Colloid Interface Sci. 300 (2006) 447–452.
[17] E.D. van Hullebusch, J. Gieteling, M. Zhang, M.H. Zandvoort, W.V. Daele, J. Defrancq, P.N.L. Lens, Cobalt sorption onto anaerobic granular sludge: isotherm and spatial localization analysis, J. Biotech. 121 (2006) 227–240.
[18] I. Smičiklas, S. Dimović, I. Plećaš, M. Mitrić, Removal of Co^{2+} from aqueous solutions by hydroxyapatite, Water Res. 40 (2006) 2267–2274.
[19] S.I. El-Dessouky, E.A. El-Sofany, J.A. Daoud, Studies on the sorption of praseodymium (III), holmium (III) and cobalt (II) from nitrate medium using TVEX–PHOR resin, J. Hazard. Mater. 143 (2007) 17–23.
[20] N.S. McIntyre, M.G. Cook, X-ray photoelectron studies on some oxides and hydroxides of cobalt, nickel, and copper, Anal. Chem. 47 (1975) 2208–2213.
[21] N.S. McIntyre, D.D. Johnston, L.L. Coatsworth, R.D. Davidson, J.R. Brown, X-ray photoelectron spectroscopic studies of thin film oxides of cobalt and molybdenum, Surf. Interface Anal. 15 (1990) 265–272.
[22] B.J. Tan, K.J. Klabunde, P.M.A. Sherwood, XPS studies of solvated metal atom dispersed (SMAD) catalysts. Evidence for layered cobalt-manganese particles on alumina and silica, J. Am. Chem. Soc. 113 (1991) 855–861.
[23] C.D. Wagner, W.M. Riggs, L.E. Davis, J.F. Moulder, G.E. Muilenberg, Handbook of X-Ray Photoelectron Spectroscopy, Perkin-Elmer Corporation, Physical Electronics Division, Eden Prairie, MN 55344, (1979).